Fuel Reformation by Piston Compression of Rich Air-Fuel Mixture

Gen Shibata[1]*, Go Asai[2], Shuntaro Ishiguro[1], Yusuke Watanabe[1], Yoshimitsu Kobashi[1], and Hideyuki Ogawa[1]

[1] Division of Energy and Environmental Systems, Graduate School of Engineering, Hokkaido University, Japan

[2] Powertrain Research Division, Research and Development Center, Yanmar CO., LTD., Japan

* Corresponding author at: Kita 13, Nishi 8, Kita-ku, Sapporo, Hokkaido, Japan

E-mail address: g-shibata@eng.hokudai.ac.jp (Gen Shibata)

Abstract

The purpose of this paper is to investigate and describe the fuel reformation by diesel piston compression to change the ignitability of commercial fuels for marine engines. The engine operational conditions were first investigated by CHEMKIN Pro with n-heptane as a fuel, an HCCI engine with port fuel injection was operated by n-heptane based on simulation results, and the production of reformed gases (hydrogen, carbon monoxide, methane, and ethylene) were measured by emission analyzers. The fuel reformation becomes active above a 2.0 equivalence ratio and higher intake air temperature conditions, and the molar fractions of the reformed gases can be varied by the maximum in-cylinder average temperature during the reforming processes.

An indirect injection diesel engine was newly introduced and the diesel fuel reformation characteristics were evaluated.

Further, the fuel decomposition processes were investigated by CHEMKIN Pro. The results suggest that the hydrogen and carbon monoxide are produced via a number of production paths in the fuel decomposition into small hydrocarbons and chemical production controls of hydrogen and carbon monoxide will be difficult. However, the production paths of methane and ethylene formation are limited by the decomposition of hydrocarbons and this suggests the possibility of chemical production control of methane and ethylene.

Keywords: Fuel Reformation, Piston Compression, Diesel Engine, Hydrogen, Carbon Monoxide, Methane, Ethylene

Nomenclature:

CF ROP	Factors contributing to the rate of production
CF Mole	Factors contributing to the molar ratios produced
CN	Cetane number

EGR	Exhaust gas recirculation
FTIR	Fourier transform infrared spectrometry
GC/MS	Gas chromatography mass spectrometry
HCCI	Homogeneous charge compression ignition
HPLC	High performance liquid chromatography
IDI	Indirect injection
RCCI	Reactivity controlled compression ignition
ROC	Rate of change
RON	Research octane number

Greek symbols:

ϕ	Equivalence ratio

1. Introduction

The fuel standards, the research octane number (RON) and cetane number (CN), are very important to avoid engine knocking, however this restricts the developments of high performance engines, because the engine must be developed along the lines of the standardized ignitability of marketed gasolines and diesel fuels. To change the fuel ignitability, RCCI research has been conducted by the Reitz research group in University of Wisconsin-Madison [1], [2]. The fuel ratio of gasoline and diesel fuel can be changed depending on the engine speed and load, and they have achieved 1.45 MPa BMEP by the RCCI operation. The RCCI combustion has the characteristics of a high degree of constant volume, and more than 50% of indicated thermal efficiency can be attained at middle load operation [3]. Further, they introduced a catalytic reforming system for the RCCI engine to generate syngas and succeeded to develop the single fuel RCCI system [4]. Hwang reported the single-fuel reactivity control by diesel fuel [5], Shudo investigated the methanol reformation to dimethyl ether [6], [7], and Yap investigated the natural gas fuel reforming [8] to change the fuel reactivity for HCCI operations. The on-board fuel reformation is more realistic than dual fuel combustion.

Tartakovsky provided an overview of the research on fuel reforming in internal combustion engines and introduced the fundamentals of fuel reforming, chemical fuel reforming, and in-cylinder reforming by piston compression and EGR [9]. In chemical fuel reforming analysis, Kopasz investigated the fuel reformation by a microreactor [10] and the results concluded that alcohols are reformed at lower temperatures, less than 600C, while complex fuels like gasoline and diesel fuel require higher temperatures, above 700C for maximum hydrogen production.

The catalytic fuel reforming of gasoline [11], [12] and diesel fuels is much investigated [13]. For passenger car engines, Ashida reported on on-board fuel reforming to avoid gasoline knocking at high load operation [14], [15]. The gasoline is injected to a catalyst in the exhaust pipe, the reformed gases of hydrogen (H_2) and carbon monoxide (CO) are recirculated to the intake port, and mixed with fresh air. The anti-knocking performance of gasoline engines at high loads was improved with the addition of generated syngas, however the exhaust temperature changes widely depending on the vehicle, and catalyst damage by sintering and hydrothermal degradation are the issues of concern here.

The main benefit of the in-cylinder reforming is the possibility of using the available engine hardware and elimination of the need for a fuel reformer. Alger at the SwRI reported the fuel reforming by a dedicated EGR (D-EGR) concept with 4 cylinder gasoline engines in 2009 [16], and Sarlashkar showed high thermal efficiency operation with low emissions in transient conditions [17]. Eyal investigated the energy conversion in a reforming-controlled compression ignition system, and exergy analysis was conducted for dimethyl ether reforming [18]. Wiemann reported the partial oxidation of methane-air mixtures with single cylinder SI and HCCI engines [19], and Hegner investigated the partial oxidation of dimethyl ether by the combustion analysis of simulations and rapid compression machine experiments [20].

In this paper, in-cylinder reforming by piston compression of a rich air-fuel mixture is a subject of the research. The target engine is a multi-cylinder marine diesel engine, which has two types of cylinders, reformer cylinder and power cylinder. The research concept is shown in Figure 1. The diesel fuel is injected in the intake port and mixed with the air-EGR gas, the fuel rich mixture is introduced to the reformer cylinders, and the reformed gases are produced by the piston compression. The reformed gases are re-mixed with fresh air, introduced to the power cylinders, and ignited by the compression ignition of a small amount of diesel fuel injection. In this system, a single fuel is used and the combustion effects similar to the dual fuel combustion with low emissions and high thermal efficiency can be achieved.

Tests with two engines were conducted in this present research: fundamental reformation tests by an HCCI engine (Nissan SC-77) with n-heptane, and applied reformation tests by an indirect injection (IDI) diesel engine (Yanmar TF 120V-E) with n-heptane and diesel fuel.

In the fundamental reformation tests, n-heptane, which has an ignitability similar to diesel fuel, was used to avoid the effects of vaporization characteristics on the fuel reforming. The decomposition and oxidation processes of n-heptane were analyzed by CHEMKIN Pro, computed chemistry dynamics software, and the reformed gas production conditions

were first investigated. The intake air temperature before compression, equivalence ratio, and compression ratio are the parameter variables, and the production of hydrogen (H_2), carbon monoxide (CO), methane (CH_4), and ethylene (C_2H_4) were calculated. The ignitability of those chemicals is lower than that of diesel fuel, however as the H_2 induces pre-ignition in high load engine operation with the increase in the equivalence ratio of H_2 [21], [22], the production of CO, CH_4, and C_2H_4 were measured and evaluated as alternatives to H_2. Then the HCCI engine was operated according to the calculation results, and the results of the reformed gas production in simulations and engine tests were analyzed.

In the applied reformation tests, the indirect injection (IDI) diesel engine (Yanmar TF 120V-E) was operated with n-heptane as a fuel, and the characteristics of the reformed gases were compared with those of the HCCI engine (Nissan SC-77) to confirm the similarities of the reformation results in the HCCI and IDI operation. Following this, the engine was operated with diesel fuel, and the diesel fuel reformation characteristics were evaluated.

Further, the elementary reactions of the reforming process were analyzed by CHEMKIN Pro, and the contributions of the elementary reactions for H_2, CO, and CH_4 production are investigated and discussed.

2. Test Methods

2.1 Calculations by Computed Chemistry Dynamics (Simulation)

2.1.1 The Analysis of Reforming Conditions for Fundamental Reformation Tests

To investigate the fuel reforming conditions of temperature and equivalence ratios, the calculations of the computed chemistry dynamics were conducted by CHEMKIN Pro. The calculation conditions are shown in Table 1. A single cylinder HCCI engine (Nissan SC-77), 85 mm bore, 88mm stroke, and compression ratio of 18.0, was used in the fundamental reformation tests as the initial setup for the calculations. The n-heptane is used as an alternative to diesel fuel to avoid the effects of vaporization characteristics on the fuel reformation in the calculations. In the simulations, the reformed gas production conditions were first investigated. The intake air temperature before the piston compression, equivalence ratio, and compression ratio were changed as parameter variables, and the production of hydrogen (H_2), carbon monoxide (CO), methane (CH_4), and ethylene (C_2H_4) were calculated. Then the HCCI engine was operated according to the calculated results.

2.1.2 Reaction Analysis of the Reformation Processes by CHEMKIN Pro. (Simulation)

To investigate the reforming processes of the fuel (n-heptane), a sensitivity analysis of the reactions was conducted. The reformed gases, H_2, CO, CH_4, and C_2H_4, are produced and consumed through numerous reactions during the reformation, and the important reactions are selected by the contributing factors of the rate of production (CF ROP) and production molar ratio (CF Mole) by CHEMKIN Pro as shown in equations 1 and 2 below, because both the production (and consumption) speed and production amounts are related. The contribution factor expresses the contribution ratio of the elementary reaction j for all the elementary reactions (the number of elementary reactions is Ni) to produce or consume a certain chemical i (H_2, CO, CH_4, or C_2H_4) in the process at time t. The elementary reactions where $CF\ ROP_{i,j,t}$ and $CF\ Mole_{i,j,t}$ are higher than 1.0% were selected.

Then the sensitivity analysis was conducted as shown in equation 3. For example, in the case of carbon monoxide (CO), the extracted reactions by the evaluation of the contributing factors are all deleted from the reactions in CHEMKIN Pro, the CO production is re-calculated, and the sensitivities of the extracted reactions are evaluated as the rate of change (ROC).

The calculation conditions are shown in Table 2. When the initial temperature is 500K, the production of H_2, CO, CH_4, and C_2H_4 are the highest at equivalence ratios (ϕ) of 2.5, 2.5, 5.0, and 8.0 respectively, and the reaction analysis of the reformation processes is conducted for each condition.

$$CF\_ROP_{i,j,t} = \frac{ROP_{i,j,t}}{\sum_{j=1}^{N_i} ROP_{i,j,t}} \times 100 \qquad (1)$$

$$CF\_Mole_{i,j,t} = \frac{Mole_{i,j,t}}{\sum_{j=1}^{N_i} Mole_{i,j,t}} \times 100 \qquad (2)$$

$CF\_ROP_{i,j,t}$: Contribution of the reaction speed of the elementary reaction j at time t to produce or consume a specific chemical i [%]

$CF\_Mole_{i,j,t}$: Contribution of the mole number of the elementary reaction j at time t to produce or consume a specific chemical i [%]

$ROP_{i,j,t}$: Production or consumption speed of elementary reaction j at time t for a specific chemical i [mol/(m^3s)]

$Mole_{i,j,t}$: Production or consumption of the number of moles of the elementary reaction j at time t for a specific chemical i [mol]

N_i: Number of elementary reactions for production and consumption of chemical i [-]

$$ROC_i = \frac{\Psi_{i,after} - \Psi_{i,before}}{\Psi_{i,before}} \times 100 \qquad (3)$$

ROC_i: Rate of change in chemical i [%]

$\Psi_{i,\ before}$: Molar ratio of chemical i before removal of key reactions [-]

$\Psi_{i,\ after}$: Molar ratio of chemical i after removal of key reactions [-]

2.2 Experimental Setup and Engine Test Conditions

Two types of engine tests were conducted in the present research, a fundamental reformation test by the HCCI engine with n-heptane (Test 1) and applied reformation tests by the indirect injection (IDI) diesel engine with n-heptane and diesel fuel (Tests 2-5).

2.2.1 Fundamental Reformation Tests with the HCCI Engine (Test 1) (Fuel: n-Heptane)

A single cylinder four stroke HCCI engine (Nissan SC-77) with an intake port fuel injection system was used to eliminate the effects of air-fuel mixture inhomogeneity on the fuel reforming characteristics. The engine specifications are shown in Table 3 and the engine setup is shown in Figure 2. In the experiments, pure nitrogen is used instead of EGR to eliminate the effects of the hydrocarbon contents in the EGR. Intake air is mixed with nitrogen in the surge tank, introduced into an intake pipe, and heated by a heater. In the experiments, n-heptane, which has an ignitability similar diesel fuel, was used to verify the simulation results. The n-heptane is injected into the intake pipe 700 mm upstream from the intake valve, well-mixed with the air-nitrogen gas, and introduced into the reformer cylinder. Then, the mixture is compressed by the piston and the reformed gases of H_2, CO, CO_2, CH_4, and C_2H_4 are analyzed by Fourier transform infrared spectrometry (FTIR) (HORIBA: MEXA-4000FT) and emission analyzers (SHIMADZU: CGT 7000, TYK: NOTORP-GH). The CO, CO_2, and CH_4 are measured by both the HORIBA MEXA-4000FT and the SHIMADZU CGT7000. The measurement errors of CO and CO_2 are below ±0.02% and the measurement error of CH_4 is below ±0.01%. The C_2H_4 is measured by the HORIBA MEXA-4000FT and calibrated by high performance liquid chromatography (HPLC), and the measurement error is below ±0.01%. The error in the TYK NOTRP-GH, the hydrogen analyzer, is below ±0.1%, calibrated by the HORIBA MSHA-1000L.

The engine speed is maintained at 1000 rpm. The compression ratio, intake air temperature, and intake oxygen concentration (or equivalence ratio) were the parameter variables, as shown in Table 4 and the engine experiments were repeated five times and

averaged in each test condition. The equivalence ratio is changed by the air/nitrogen ratio maintaining the fuel injection quantity.

2.2.2 Applied Reformation Tests with the IDI Diesel Engine (Tests 2-4) (Fuel: n-Heptane)
The achievement of diesel fuel reforming is one of the objects of the research here and a single cylinder engine (Yanmar TF 120V-E in Table 3) was newly introduced. This engine can be operated by direct injection (DI) or indirect injection (IDI) by the change of cylinder heads, and the fuel reformation by DI and IDI operations were first investigated separately. To make a uniform air-fuel mixture, the fuel must be injected at early timings, however the results in DI operation showed an increase in engine oil dilution by the fuel because much fuel impinged on the cylinder walls. If the fuel injection timing is retarded to earlier than 30 CA BTDC, the smoke emissions increase. Based on the pre-tests of DI and IDI engine operations, we concluded that the DI diesel engine is not suitable for fuel reformation and the experiments in the applied reformation tests were conducted by the single cylinder IDI diesel engine. The IDI diesel engine has a low pressure (20MPa) two hole injector to prevent fuel spray penetration from sub-chamber to main-chamber. The engine setup is the same as that in Figure 2. The injection timing and injection pressure of the n-heptane were maintained at 40 CA BTDC and 20MPa respectively.
The IDI diesel engine was operated with n-heptane and the reformed gas production characteristics are compared with those of an HCCI engine (Nissan SC-77) to ensure the similarities of the reformation results in the HCCI and IDI operation. The test conditions in Test 2 are shown in Table 5. In Test 2, the equivalence ratio is changed by the air quantity maintaining the fuel injection quantity.
In Test 3, 1.5 times of the base fuel in Test 2 were injected and the equivalence ratio was changed according to the conditions of the air/nitrogen quantity with the basic conditions in Test 2, as show in Table 6, and the production of H_2, CO, CH_4, and C_2H_4 were analyzed.
In Test 4, the engine speed was changed from 800 to 1200 rpm to investigate the effects of the reaction duration on the reformed gas production. The test conditions are shown in Table 7.

2.2.3 Effects of Fuel Injection Timing on the Reformed Gas Production by the IDI Diesel Engine (Test 5) (Fuel: Diesel Fuel and n-heptane)
In Test 5, the reformation characteristics of the diesel fuel were investigated with the IDI diesel engine. The diesel fuel properties used in the experiments are shown in Table 8. As the diesel fuel vaporization characteristics affect the reformation efficiency, the fuel injection timing (-130, -100, and -70 CA ATDCs) and equivalence ratio (4.0-8.0) were

the parameter variables in Test 5, as shown in Table 9.

3. Results and Discussion

3.1 Fuel Reformation Conditions of the Temperature and Equivalence Ratio (Simulation)

To determine the fuel reformation conditions of the temperature and equivalence ratio, calculations by the computed chemistry dynamics, CHEMKIN Pro, were conducted. In the research here, we focused on the four reformed gases, hydrogen (H_2), carbon monoxide (CO), methane (CH_4), and ethylene (C_2H_4). The ignitability of those gases is lower than diesel fuel, however as the H_2 induces pre-ignition in high load engine operation with the increase in the equivalent ratio of H_2, the production of CO, CH_4, and C_2H_4 were evaluated as alternatives to H_2. In the reforming processes, water (H_2O) and carbon dioxide (CO_2) are produced and monitored to evaluate the production balance with H_2 and CO. The soot emissions were not evaluated by simulations here, however it will be evaluated by the engine experiments below.

The calculated results are shown in Figure 3. The ordinate and abscissa show the intake air temperature before piston compression and equivalence ratio respectively. The gray area in each figure shows the non-reactive equivalence ratio and temperature (ϕ-T) areas. As the air-fuel mixture becomes richer, the reformation occurs at higher temperatures. Under the 1.5 equivalence ratio condition, much of CO_2 and H_2O are produced and fuel reformation to H_2, CO, C_2H_4, and CH_4 does not occur because the n-heptane combusts well here. For H_2 and CO, the equivalence ratio of 2.0-4.0 is suitable and the production increases with the increase in the initial temperature, however for C_2H_4 and CH_4, the equivalence ratios for reformation are much richer than those for H_2 and CO. An equivalence ratio higher than 5.0 is necessary for CH_4 and an equivalence ratio higher than 8.0 is necessary for C_2H_4.

3.2 Fundamental Reformation Tests by the HCCI Engine (Test 1) (Fuel: n-Heptane)

Based on the simulation results in section 3.1, the HCCI engine was operated. As the temperature is an important factor to change the yields of reforming gases, the compression ratio and the intake air temperature by pre-heating were changed in the engine experiments especially in Tests 1 and 2. (Here, the intake air was heated by an electric heater, however if it is applied to marine engine systems, the pre-heating can be achieved by a heat exchanger in the exhaust in the power cylinder, as shown in Figure 1.)

Further, it was found that the soot emission level is the highest at the 2.0 equivalence ratio, however if the equivalence ratio is higher than 2.5, soot is not emitted. From these

test results, the engine was generally operated under the conditions of 2.0-3.3 equivalence ratios for compression ratios of 16.0 and 18.0 (for the compression ratio of 20, the engine tests were conducted at 2.5-5.0 equivalence ratio conditions) and 400-500 K initial temperature, as listed in Table 4.

The HCCI engine tests were conducted under three different compression ratio conditions (16,0, 18.0, and 20.0), and the intake air temperature and oxygen concentration (equivalence ratio) are the test parameter variables. The ignitability of H_2, CO, CH_4, and C_2H_4 is lower than that of diesel fuel, however as the H_2 is a cause of preignition in high load operation of the power cylinder, the production of CH_4 and C_2H_4 are used as alternatives to H_2.

The test results are shown in Figure 4. The reformed gas production of H_2, CO, CH_4, and C_2H_4 can be arranged by the maximum in-cylinder average temperature during the reformation processes. Figure 4 (a) shows the H_2 production characteristics and there is a linear relation with the maximum in-cylinder average temperature. Figure 4 (b) shows the production characteristics of CO and CO_2, there is an inflection point around 1200-1250 K because the CO starts to be oxidized to CO_2 above this temperature range. In Figure 4 (c), the peak production temperatures of CH_4 and C_2H_4 were observed at 1200 and 1000K respectively, and these results suggest that the CH_4 and C_2H_4 production increases with the increase in the maximum in-cylinder average temperature, however these two compounds decompose into H_2 and CO above the peak temperatures. The reason why the peak temperature of CH_4 is higher than that of C_2H_4 is because of the stiffness of the tetrahedral structure of CH_4.

The reformed gases were analyzed by Fourier transform infrared spectrometry (FTIR), gas chromatography mass spectrometry (GC/MS), and high performance liquid chromatography (HPLC), and the gas compositions are shown in Figure 5. The total molar fraction of CO_2, H_2O, CO, H_2, and hydrocarbons (CH_4-C7 HCs) increases with the increase in intake oxygen concentration (decrease in equivalence ratio), however each reformed gas production characteristic is different. Much H_2, CO, and CO_2 is produced at the conditions of the higher intake oxygen concentrations, and the CH_4 and hydrocarbons at conditions of lower intake oxygen concentrations. These tendencies are similar to the simulation results in Figure 3.

Figure 6 shows the composition of hydrocarbons in the reformed gases in Test 1. The underlined numbers in the columns represent the total hydrocarbons, and the composition is shown with the pie chart. With the decrease in oxygen concentration, the total hydrocarbon increases, the production ratio of CH_4 decreases, and the ratio of C_2H_4 increases with the initial gas temperature.

The sum of the lower heating values of reformed gases is shown in Figure 7. With the decrease in intake oxygen concentration in the intake air temperature, the total heating value of H_2 and CO decreases, however the heating value contribution of CH_4, C_2H_4, and higher hydrocarbons (C3-C7 and over) increases and the total heating value increases. Under the same conditions of intake oxygen concentration, the sum of the H_2 and CO heating values is constant at the 400 K, 450 K, and 500 K conditions, however the sum of the CH_4 and C_2H_4 heating values increases with the decrease in intake air temperature. The previously published research in [16], [17] suggests the yield of the different gases by in-cylinder reformation and this was confirmed in our engine tests. More of H_2 and CO are produced when the intake oxygen concentration is higher, however more of CH_4 and C_2H_4 are produced when the intake oxygen concentration and intake air temperatures are lower, as shown by Figure 7.

3.3 Applied Reformation Tests with the IDI Diesel Engine (Tests 2-4) (Fuel: n-Heptane)

3.3.1 Fuel Reformation by the IDI Engine (Test 2)

In the applied reformation tests, a single cylinder indirect injection (IDI) diesel engine (Yanmar TF 120V-E) was newly introduced to enable fuel reformation by diesel fuel. In the tests here, the IDI diesel engine was operated with n-heptane fuel and the production characteristics of the reformed gases are compared with those of the HCCI engine (Nissan SC-77) to confirm the similarities of reformation results in the HCCI and IDI operations. The test conditions are shown in Table 5. There were no soot emissions because the equivalence ratio is higher than 2.5 for all test conditions, the extremely high-fuel-rich mixture.

The test results are shown in Figure 8. There is no difference in the H_2 production of the HCCI and IDI engines (Figure 8 (a)), however as in Figures 8 (b)-(e), the fuel reformation to CO, CO_2, CH_4, and C_2H_4 in the IDI engine occurs at higher temperatures than those in the HCCI engine, and the production peaks of the production of CH_4 and C_2H_4 are higher than those of the HCCI engine. The quantitative tendencies of the CO, CO_2, CH_4, and C_2H_4 formation in the HCCI and IDI engines are not the same, however the qualitative tendencies are very similar for both engines. As the higher production of CH_4 and C_2H_4 were shown by the IDI engine with n-heptane, the diesel fuel reformation in Test 5 was conducted with the IDI engine.

3.3.2 Effects of Fuel Injection Quantity on Reformed Gas Production (Test 3)

In Test 3, 1.5 times of the base fuel in Test 2 was injected and the equivalence ratio changed according to the conditions of the air/nitrogen quantity with the base conditions

in Test 2, as detailed in Table 6, and the production of H_2, CO, CH_4, and C_2H_4 as shown in Figure 9 were analyzed.
In Figure 9, the open plots show the test results of the base fuel injection and the solid plots show the test results with the 1.5 times base fuel injection. In Figure 9 (a)-(d), the production of reformed gases, the H_2, CO, CH_4, and C_2H_4, were all higher with the increases in fuel injection quantity.

3.3.3 Effects of Engine Speed on Reformed Gas Production (Test 4)
The engine speed was changed from 800 to 1200 rpm to investigate the effects of the reaction duration on the reformed gas production in Test 4. In this test, 1.5 times of the base fuel in Test 2 were injected. The test conditions and results are shown in Table 7 and Figure 10 respectively. The high temperature retention time becomes shorter with the increase in engine speed, however there is no effect of engine speed on the produced amounts of the reformed gases, and this shows that the reformed gas reaction is fast enough and completed even at the 1200 rpm engine speed. This result suggests that the produced amounts cannot be increased by engine rotation speeds below 1200 rpm. The engine experiments were not conducted above 1200 rpm, because the maximum engine speed of the target marine engine is lower than 1200 rpm. If the engine speed were higher than 1200 rpm, the chemical reaction speed is still high enough, however the air-fuel mixing is not sufficient and the mixture inhomogeneity will also affect the production of reformed gases, especially for CH_4 and C_2H_4.

3.4 Effects of Fuel Injection Timing on Reformed Gas Production by the IDI Diesel Engine (Tests 5) (Fuel: Diesel Fuel and n-Heptane)
The reformation characteristics of diesel fuel were investigated with the IDI diesel engine in Test 5. The test conditions are shown in Table 9. As it is considered that the diesel fuel vaporization characteristics affect the reformation efficiency, the fuel injection timings (-70, -100, and -130 CA ATDC) were chosen as a parameter variable in Test 5 and the reformation characteristics of n-heptane and diesel fuel are both plotted in Figure 11, and the test data is shown in Tables 10 and11. Tables 10 and 11 show that the maximum in-cylinder temperature of diesel fuel is always higher than that of n-heptane at the same test conditions of fuel injection timing and intake O_2 concentration, and the H_2 production of diesel fuel is higher than that of n-heptane. However, if the data is arranged by the maximum in-cylinder temperature as in Figure 11 (a), the produced quantity of H_2 from the diesel fuel is smaller than that of n-heptane. In Figure 11 (b), the production of CO from diesel fuel and n-heptane were similar. The results of H_2 and CO suggest that the

fuel distillation and H/C ratio may change the combustion characteristics of each fuel and affect the reformation characteristics of H_2 and CO.

In Figures 11 (c) and (d), the production of CH_4 and C_2H_4 from diesel fuel is lower than from n-heptane. Compared with n-heptane, the volatility and molecular size of diesel fuel are higher and longer, and the differences in the vaporization characteristics may affect the production of CH_4 and C_2H_4. The fuel injection timing with n-heptane affects the production of the CH_4 and C_2H_4 reformed gases slightly. In Figures 11 (c) and (d), the production of CH_4 and C_2H_4 from n-heptane decreases with the delay in the fuel injection timing. The histories of the pressure and tumble ratios during the compression stroke is shown in Figure 12. The tumble ratio is defined as the number of in-cylinder gas tumble rotations in the sub-chamber per engine rotation. The in-cylinder pressures at -130, -100, -70, -40, and -10 CA ATDCs during compression are 0.13, 0.18, 0.32, 0.90, 3.81 MPa respectively and the tumble ratio increases as the piston approaches the TDC. If the fuel is injected at the -100 or -130 CA ATDC condition, the air tumble rotation speed in the sub-chamber is slow and the air-fuel mixing is not sufficient for a complete mixing. In the experiments of diesel fuel reformation, more soot was emitted in the exhaust than with n-heptane and the maximum temperature of the diesel fuel is higher than that of n-heptane, as shown in Tables 10 and 11. This suggests that the diesel fuel adheres to the walls and forms a fuel film on the surface of the sub-chamber, as shown in Figure 13, and the diesel fuel combusts in a leaner state than the n-heptane. The distillation of diesel fuel affects the heterogeneity of the air-fuel mixture in the cylinder.

There is an optimum fuel injection timing for n-heptane at -70 to -40 CA ATDC, for the production of CH_4 and C_2H_4. In the experiment, if the fuel injection is later than -40 CA ATDC, the performance of the fuel reformation worsens and the soot production increases, because there is not sufficient time for the reformation. These results suggest that a high tumble ratio in the sub-chamber and a sufficient time for air-fuel mixing are necessary for the fuel reformation in IDI diesel engines.

3.5 Reaction Analysis of the Reformation Processes by CHEMKIN Pro.

The elementary reactions whose $CF\ ROP_{i,j,t}$ and $CF\ Mole_{i,j,t}$ in equations 1 and 2 are higher than 1.0% were selected. The main reactions of calculated results are discussed here, and the details of production and consumption reactions are shown in Appendix 1.

3.5.1 The Main Reactions of Production/Consumption of Hydrogen (H_2)

The basic reaction is shown in R1, dehydrogenation by the hydrogen radical (H), and the R2-R5 are examples of the main reactions. The dehydrogenation commonly occurs in the reforming processes and contributes to the production of H_2 and H_2O. The R2 and R3 are

H_2 production reactions, and the R4 and R5 are H_2 production and consumption reactions.

$RH + H \leftrightarrow R + H_2$ (R1) (Basic reaction)

$H_2 + OH \leftrightarrow H + H_2O$ (R2) (Production)
$CH_2O + H \rightarrow HCO + H_2$ (R3) (Production)
$C_2H_4 + H \leftrightarrow C_2H_3 + H_2$ (R4) (Production and consumption)
$CH_4 + H \leftrightarrow CH_3 + H_2$ (R5) (Production and consumption)

3.5.2 The Main Reactions of Production/Consumption of Carbon Monoxide (CO)
The basic reaction is shown in R6, that is the dissociation reaction of the carbonyl radical (-CO), and R7-R10 are examples of the main reactions. The dissociation reaction also commonly occurs in the reforming processes and contributes to the productions of CO. The reaction proceeds to CO_2 under high temperature and O_2 rich conditions. The R7, R8, and R9 are the CO production reactions, and R10 is the CO consumption reaction.

$RCO \leftrightarrow R + CO$ (R6) (Basic reaction)

$HCO + M \leftrightarrow H + CO + M$ (R7) (Production)
$CH_3CO + M \rightarrow CH_3 + CO + M$ (R8) (Production)
$CH_2CO + H \leftrightarrow CH_3 + CO$ (R9) (Production)

$CO + OH \leftrightarrow CO_2 + H$ (R10) (Consumption)

3.5.3 The Main Reactions of Production/Consumption of Methane (CH_4)
The basic reaction is shown in R11, dehydrogenation by the methyl radical (CH_3), and R12-R16 are examples of the main reactions. The reactions in R12-15 are the CH_4 production reactions, and the R12 and R15 are dominant. The R16 is a CH_4 consumption reaction.

$RH + CH_3 \leftrightarrow R + CH_4$ (R11) (Basic reaction)

$CH_4 + H \leftrightarrow CH_3 + H_2$ (R12) (Production)
$C_5H_6 + CH_3 \leftrightarrow C_5H_5 + CH_4$ (R13) (Production)
$C_2H_4 + CH_3 \leftrightarrow C_2H_3 + CH_4$ (R14) (Production)
$CH_4 + OH \leftrightarrow CH_3 + H_2O$ (R15) (Production)

$CH_4 + H \leftrightarrow CH_3 + H_2$ (R16) (Consumption)

3.5.4 The Main Reactions of Production/Consumption of Ethylene (C_2H_4)

The basic reaction is shown in R17, the thermal decomposition of higher hydrocarbons, and R18-R27 are examples of the main reactions. The R18-R23 are C_2H_4 production reactions and the R24-R27are C_2H_4 consumption reactions.

$R \leftrightarrow C_2H_4 + R'$ (R17) (Basic reaction)

$C_7H_{15} \leftrightarrow C_5H_{11} + C_2H_4$ (R18) (Production)
$C_5H_{11} \leftrightarrow C_3H_7 + C_2H_4$ (R19) (Production)
$C_3H_7 \leftrightarrow C_2H_4 + CH_3$ (R20) (Production)
$C_4H_9 \leftrightarrow C_2H_5 + C_2H_4$ (R21) (Production)
$C_2H_5 + M \leftrightarrow H + C_2H_4 + M$ (R22) (Production)
$C_5H_5 + O_2 \leftrightarrow HO_2 + C_2H_4$ (R23) (Production)

$C_2H_4 + O \leftrightarrow CH_3 + HCO$ (R24) (Consumption)
$C_2H_4 + O \leftrightarrow CH_2CHO + H$ (R25) (Consumption)
$C_2H_4 + OH \leftrightarrow C_2H_3 + H_2O$ (R26) (Consumption)
$C_2H_4 + CH_3 \leftrightarrow C_2H_3 + CH_4$ (R27) (Consumption)

The ethylene (C_2H_4) is produced from C_7H_{15} (R18), C_3H_7 (R20), C_4H_9 (R21), and C_2H_5 (R22 and R23), and when the C_7H_{15}, C_3H_7, C_4H_9, and C_2H_5 are produced, hydrogen (H_2) and carbon monoxide (CO) are produced as shown in the R28-32 reactions.

Hydrogen production

$C_7H_{16} + H \leftrightarrow C_7H_{15} + H_2$ (R28) (Production)
$C_3H_8 + H \leftrightarrow C_3H_7 + H_2$ (R29) (Production)

Carbon monoxide production

$C_3H_7CO \leftrightarrow C_3H_7 + CO$ (R30) (Production)
$C_4H_9CO \leftrightarrow C_4H_9 + CO$ (R31) (Production)
$C_2H_5CO \leftrightarrow C_2H_5 + CO$ (R32) (Production)

3.5.5 Possibility for Active Production Controls of Reformed Gas Amounts

The sensitivity analysis expressed in equation 3 above was conducted. For instance, with the CO, the main reactions of CO production and consumption in Figures AP-2, are all removed from the reactions in CHEMKIN Pro and the production of CO is re-calculated. According to equation 3, the rate of change in CO was 7.8% as shown in Figure 14. This suggests that the CO is easily produced from other elementary reactions even if the elementary reactions in Tables AP-2 in Appendix are all removed. In the case of H_2, the rate of change was 31.6%, higher than CO but lower than the rates of change in CH_4 (85.1%) and C_2H_4 (92.7%). This suggests that there are many production paths for CO and H_2, however for CH_4 and C_2H_4, the elementary reactions in Tables AP-3 and AP-4 in Appendix are the main reactions for the production of CH_4 and C_2H_4.

A diagram of the detailed reaction paths were analyzed by CHEMKIN Pro. As shown in Figure 15, there are four reaction stages: low temperature oxidation (LTO), pre-thermal ignition (PTI), thermal ignition (TI), and after-thermal ignition (ATI). The CF ROP and CF Mole in equations 1 and 2 were calculated for H_2, CO, CH_4, and C_2H_4, as shown in Figures 16-19. Figures 16 and 17 shows the H_2 and CO production and consumption. The production and consumption of H_2 and CO start from low temperature oxidation (LTO) and end at the end of the after-thermal ignition (ATI). In the LTO duration, the H_2 and CO are produced from higher hydrocarbons, and as the fuel reforming proceeds to PTI, TI, and ATI, the size of the hydrocarbons become smaller and the H_2 and CO are produced from small and medium hydrocarbons; CO is simultaneously consumed by the R10 reaction. For the H_2 production, the R2 and R28 are the governing reactions, and the R7-10 and R30-31 are the governing reactions for CO.

Figure 18 and 19 show the CH_4 and C_2H_4 production and consumption. The production of CH_4 and C_2H_4 starts from pre-thermal ignition (PTI) and ends after-thermal ignition (ATI). The fuel, n-heptane (C_7H_{16}), mostly breaks down into smaller hydrocarbons in PTI and TI, and the CH_4 and C_2H_4 are produced. For the CH_4 productions, the R12, R14, R15, and R16 are the governing reactions. For the C_2H_4, the R18-23 are production reactions, however the consumption of C_2H_4 in the R 24-27 are the rate-determining reactions

Figure 20 summarizes the reforming processes of the fuel. At the LTO and PTI periods before ignition, the H radical in n-heptane first reacts with the radicals (OH, H, O_2, and others.), and the n-heptane decomposes into small and medium sized hydrocarbons through oxidation reactions and scissions of molecules, and H_2 and CO are produced. Once the pre-thermal ignition starts, the C1-C3 hydrocarbons including CH_4 and C_2H_4 are produced and the C1-C3 hydrocarbons are decomposed into H_2 and CO in the thermal ignition process (TI). There are many production paths for H_2 and CO, however, the C_2H_4 and CH_4 production occurs after the low temperature oxidation processes with limited

production paths. This result suggests that the chemical production controls of H_2 and CO are difficult and the production of H_2 and CO must be physically controlled by the temperature and equivalence ratio, however this does offer the possibility of chemical production control for CH_4 and C_2H_4.

4. Conclusions

In this research, the fuel reformation by piston compression in diesel engines was investigated with both calculations and experiments. The hydrogen (H_2), carbon monoxide (CO), methane (CH_4), and ethylene (C_2H_4) were mainly analyzed as reformed gases. The conclusions may be summarized as follows:

1. The fuel reformation can be controlled by the intake oxygen concentration and intake air temperature. The yields of H_2 and CO become highest when the equivalence ratio is 2.0, and a higher intake air temperature maximizes the yield of H_2 and CO. The yields of CH_4 and C_2H_4 increase as the intake air temperature and equivalence ratios increase, however the equivalence ratio cannot be lower than 2.5 because of smoke emissions.
2. At all compression ratios and engine speeds, the yields of reformed gases can be achieved by the maximum in-cylinder average temperature during the piston compression and expansion strokes. For H_2 and CO, the yields increase with increases in the maximum in-cylinder average temperature, however the CO has an inflection point at 1200-1250K where the CO oxidization to CO2 starts. The CH_4 and C_2H_4 have the peak production temperatures around 1000K and 1200K respectively. The CH_4 and C_2H_4 start to decompose into H_2 and CO above the peak temperatures.
3. The IDI engine experiments with n-heptane and diesel fuel show the in-cylinder temperature and the heterogeneity of air-fuel mixture in the cylinder affects the fuel reformation characteristics.
4. As the reforming reaction speed below 1200 rpm is high, the reformed gas amounts cannot be controlled by low engine speed. At higher engine speed operation, the air-fuel mixture inhomogeneity will affect the productions of the reformed gases.
5. The governing reactions of H_2, CO, CH_4, and C_2H_4 gases were identified. The basic reaction of H_2 generation is the dehydrogenation by H radicals (R1 reaction), and the basic reaction of CO is the dissociation reaction of the carbonyl radical (R6 reaction). The production of H_2 and CO starts from low temperature oxidation (LTO) and ends after-thermal ignition (ATI).
6. The basic reaction of CH_4 is the dehydrogenation by the methyl radical (CH_3) (R11 reaction), and the basic reaction of C_2H_4 is the thermal decomposition of higher

hydrocarbons (R17 reaction). The production of CH_4 and C_2H_4 start from the pre-thermal ignition (PTI).

7. The reaction analysis of the reformation processes shows that the H_2 and CO react along numerous elementary reaction paths. This suggests that chemical production controls for H_2 and CO are difficult and that the production of H_2 and CO must be physically controlled by the temperature and equivalence ratio.
8. The production paths to CH_4 and C_2H_4 are very limited and involve the decomposition of small and medium sized hydrocarbons, suggesting the possibility of chemical production control.

Acknowledgment

This work was supported by JSPS KAKENHI Grant Number JP 21K03890. (Grant-in-Aid for Scientific Research in Japan)

References

[1] Hanson, R., Kokjohn, S., and Reitz, R., "Effects on Reactivity Controlled Compression Ignition (RCCI) Combustion at Low Load", SAE Technical Paper, 2011-01-0361, 2011

[2] Splitter, D., Hanson, R., Kokjohn, S., and Reitz, R., "Reactivity Controlled Compression Ignition (RCCI) Heavy-Duty Engine Operation at Mid- and High-Loads with Conventional and Alternative Fuels", SAE Technical Paper, 2011-01-0363, 2011

[3] Splitter, D., Wissink, M., DelVescovo, D., and Reitz, R., "RCCI Engine Operation Towards 60% Thermal Efficiency", SAE Technical Paper, 2013-01-0279, 2013

[4] Dal Forno Chuahy, F., and Kokjohn, S., "System and Second Low Analysis of the Effects of Reformed Fuel Composition in "Single" Fuel RCCI Combustion", SAE International Journal of Engines, 11(6): 861-878, 2018

[5] Hwang, J., Kane, S., and Northrop, W., "Demonstration of Single-Fuel Reactivity Controlled Compression Ignition using Reformed Exhaust Gas Recirculation", SAE Technical Paper, 2018-01-0262, 2018

[6] Shudo, T., Shima, Y., and Fujii, T., "Production of dimethyl ether and hydrogen by methanol reforming for an HCCI engine system with waste heat recovery – Continuous control of fuel ignitability and utilization of exhaust gas heat", Internatinal Journal of Hydrogen Energy, Volume 34, Issue 18, Page 7638-7647, 2009

[7] Shudo, T., "Ignition control in the HCCI combustion engine system fueled with methanol reformed gases", Journal of KONES, Internal combustion engines, 2005, 12 (3-4): 233-244

[8] Yap, D., Peucherete, M., Megaritis, A., Wyszynski, A., and Xu, H., “Natural gas HCCI engine operation with exhaust gas fuel reforming”, International Journal of Hydrogen Energy, Volume 31, Issue 5, Page 587-595, 2006

[9] Tartakovsky, L., and Sheintuch, M., “Fuel reforming in internal combustion engines”, Progress in Energy and Combustion Science, 67 (2018) 88-144

[10] Kopasz, J., Wilkenhoener, R., Ahmed, S., Carter, J., and Krumpelt, M., “Fuel Flexible Reforming of Hydrocarbons for Automotive Applications”, Advances in Hydrogen Energy, pp 47-56, 2002, https://doi.org/10.1007/0-306-46922-7_4

[11] Al-Musa,A., Al-Saleh, M., Ioakeimidis, Z., Ouzounidou, M., Yentekakis, I., Konsolakis, M., and Marnellos, G., “Hydrogen production by iso-octane steam reforming over Cu catalysts supported on rare earth oxides (REOs)”, International Journal of Hydrogen Energy, Volume 39, Issue 3, Page 1350-1363, 2014

[12] Kaltshmitt, T., Diehm, C., and Deutschemann, O., “Catalytic Partial Oxidation of Isooctane to Hydrogen on Rhodium Catalysts: Effect of Tail-Gas Recycling”, Industrial & Enginerring Chemistry Research, 2012,51,22, 7536-7546

[13] Sher, I., and Sher, E., “A novel internal combustion engine utilizing internal hydrogen production for improved efficiency – A theoretical concept”, International Journal of Hydrogen Energy, Volume 39, Issue 33, Page 19182-19186

[14] Ashida, K., Hashino, M., Maeda, H., Araki, T., Hiraya, K., and Yasuoka, M., “Study of Reformate Hydrogen-added Combustion in a Gasoline Engine”, SAE Technical Paper 2015-01-1952, 2015

[15] Ashida, K., Maeda, H., Araki, T., Hoshino, M., Hiraya, K., and Yasuioka, M., “Study of Hydrogen Additive High EGR Combustion for Gasoline Engine with Fuel Reformer”, JSAE Transaction paper, Vol. 46, No. 4, p 743-748, July 2015

[16] Alger, T., and Mangold, B., “Dedicated EGR: A New Concept in High Efficiency Engines”, SAE International Journal of Engines V118-3EJ, 2009-01-0694, 2009

[17] Sarlashkar, J., Rengarajan, S., and Roecker, R., “Transient Control of a Dedicated EGR Engine”, SAE Technical Paper 2016-01-0616. 2016

[18] Eyal, A., and Tartakovsky, L., “Second-low analysis of the reforming-controlled compression ignition”, Applied Energy, Volume 263, 114622, 2020

[19] Wiemann, S., Hegner, R., Atakan, B., Schulz, C., and Kaiser, S., “Combined production of power syngas in an internal combustion engine – Experiments and simulations in SI and HCCI mode”, Fuel, Volume 215, Page 40-45, 2018

[20] Hegner, R., Werler, M., Schibl, R., Maas, U., and Atakan, B., “Fuel-Rich HCCI Engines as Chemical Reactors for Polygeneration: A modeling and experimental Study on Product Pecies and Thermodynamics”, Energy and Fuels, 2017, 31, 12,

14079-14088
[21] Barbir, F., Basile, A., and Veziroglu, N., “Compendium of Hydrogen Energy: volume 3: Hydrogen Energy Conversion”, https://doi.org/10.1016/C2014-0-02674-3
[22] Aksu, C., Kawahara, N., Tsuboi, K., Kondo, M., and Tomita, E., “Extension of PREMIER combustion operation range using split micro pilot fuel injection in a dual fuel natural gas compression ignition engine: A performance-based and visual investigation”, Fuel, Volume 185, 243-253, 2016

Appendix 1 The Main Reactions of Production and Consumption of Hydrogen, Carbon Monoxide, Methane, and Ethylene

The elementary reactions whose $CF\ ROP_{i,j,t}$ and $CF\ Mole_{i,j,t}$ in equations 1 and 2 are higher than 1.0% were selected. The calculated results of hydrogen, carbon monoxide, methane, and ethylene are shown in Tables AP-1, AP-2, AP-3, and AP-4 respectively.

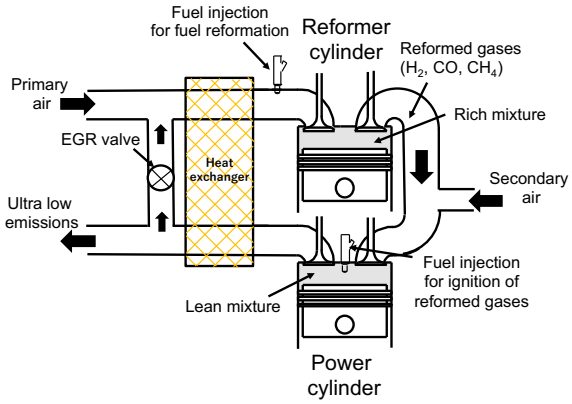

Fig. 1 Set-up for the fuel reformation concept by piston compression

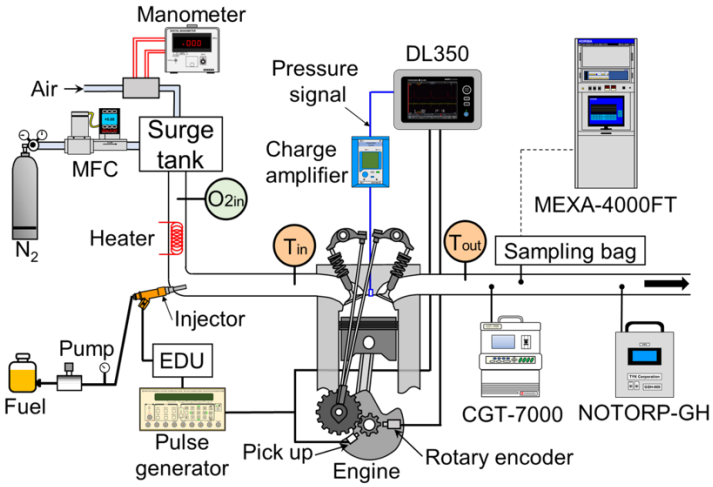

Fig. 2 Engine bench set-up

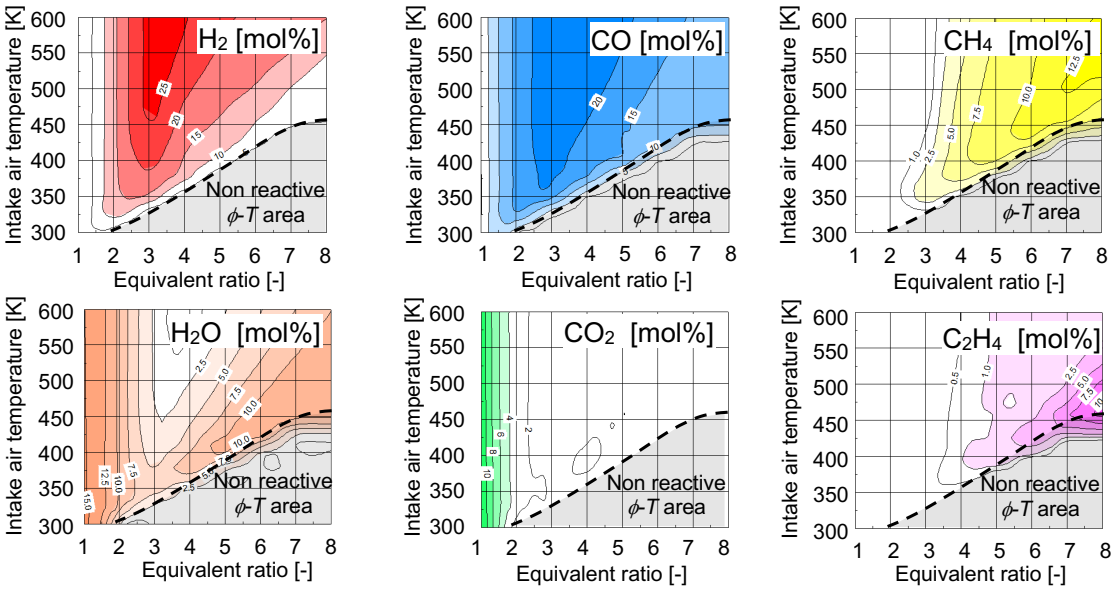

Fig. 3 Reformed gas production vs equivalent ratio and intake air temperature (simulation)

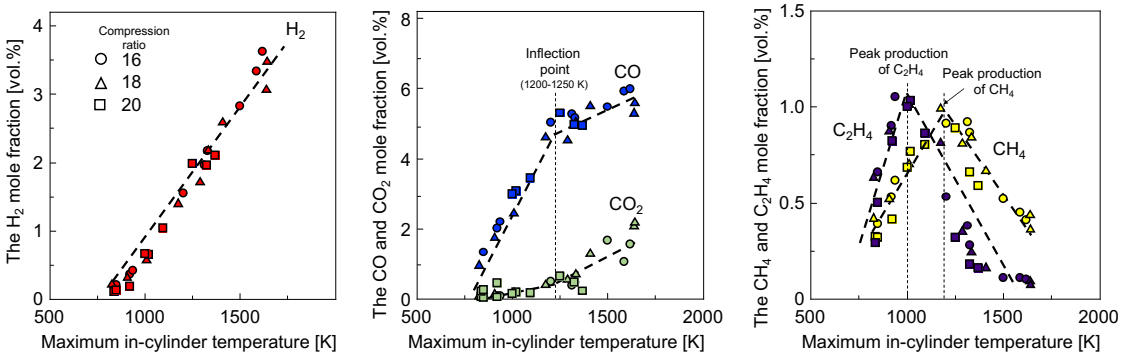

(a) Production of hydrogen (b) Production of carbon monoxide and carbon dioxide (c) Production of ethylene and methane

Fig. 4 Characteristics of reformed gas production of H_2, CO, CO_2, CH_4, and C_2H_4 (Test 1, for the HCCI engine)

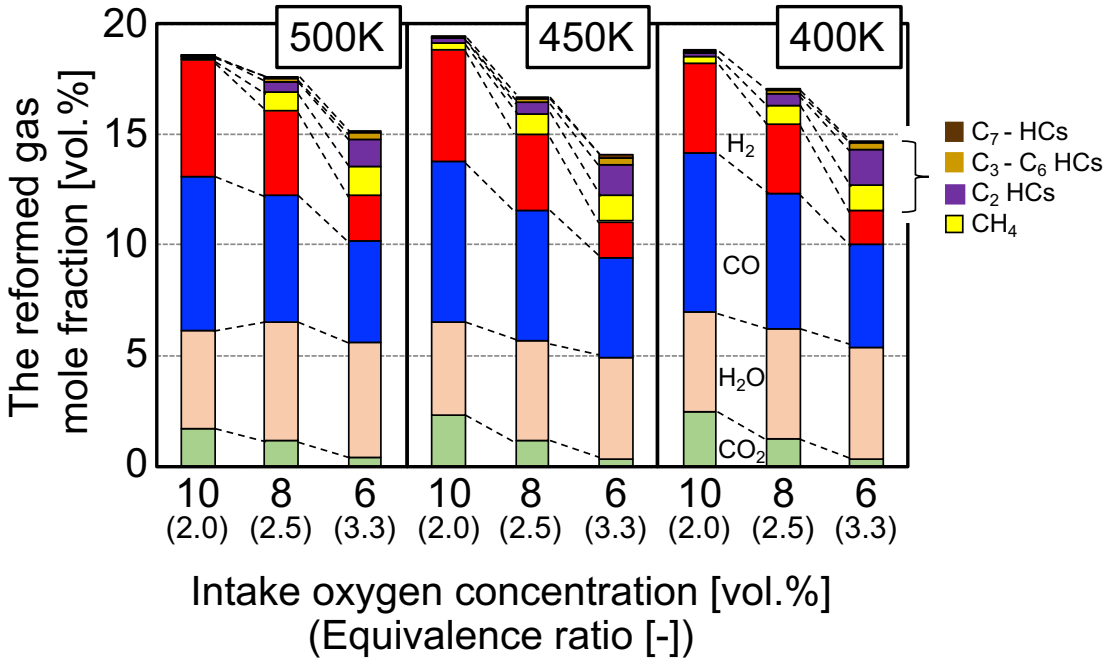

Fig. 5 Molar fractions of reformed gases (Test 1, for the HCCI engine)

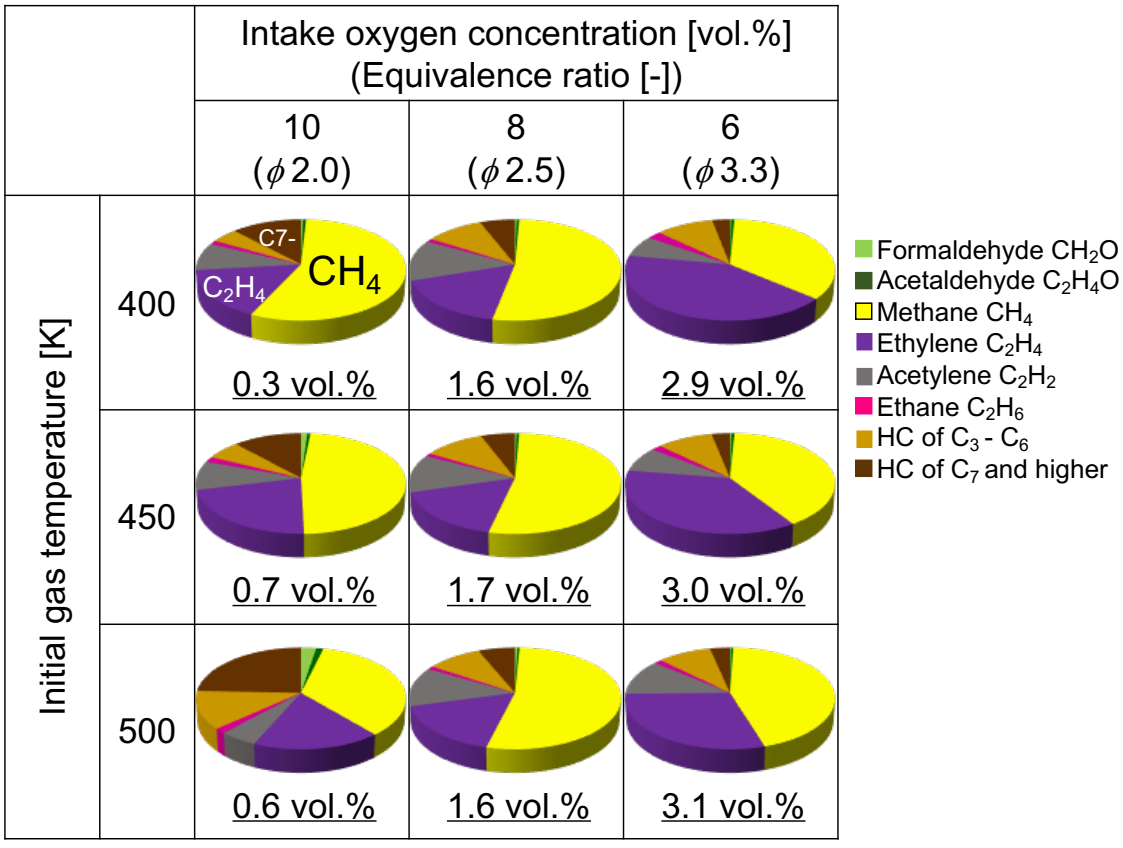

Fig. 6 Hydrocarbon components in the reformed gases (Test 1, for the HCCI engine)

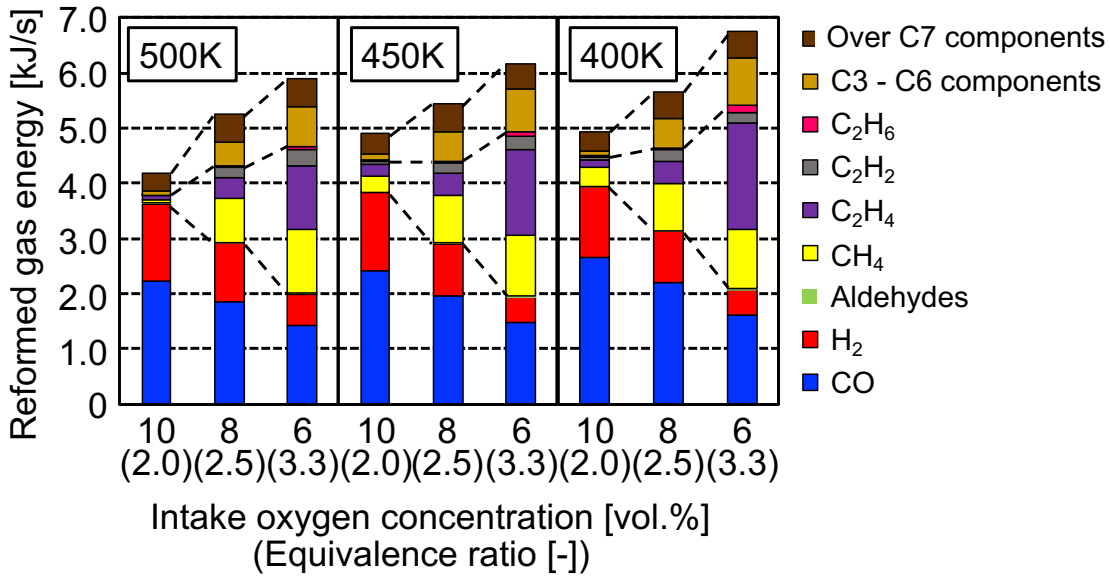

Fig. 7 Reformed gas energy (Test 1, for the HCCI engine)

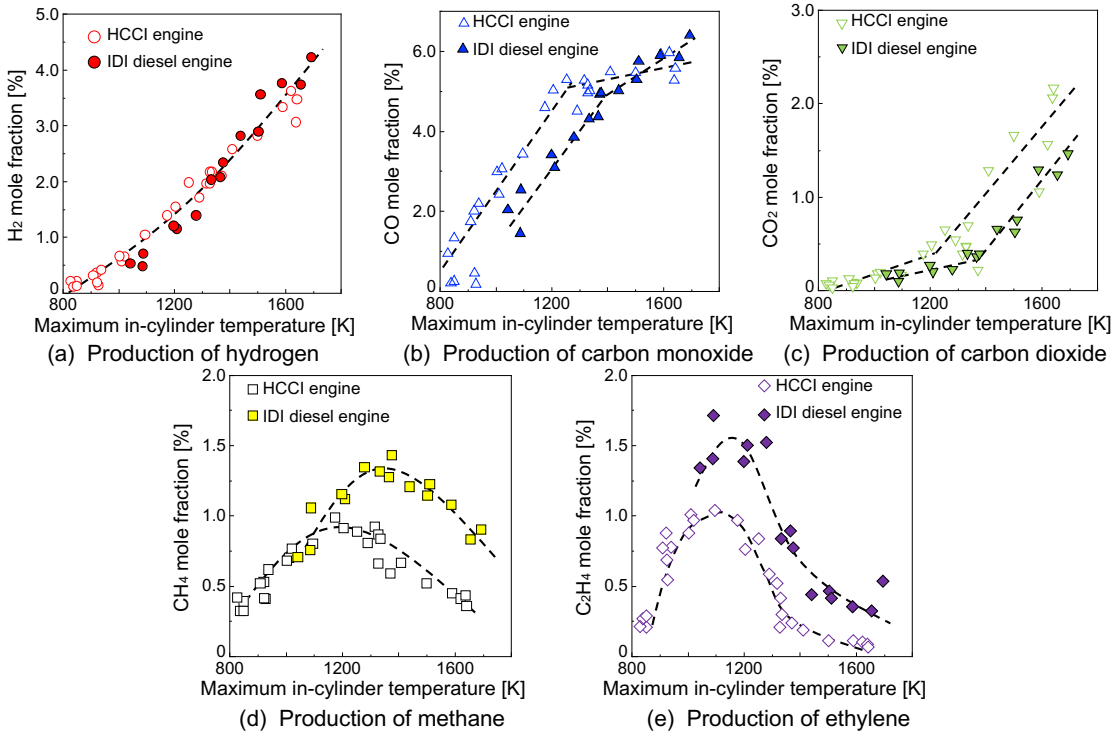

Fig. 8 Plots of reformed gas production by the HCCI and IDI engines (Test 2)

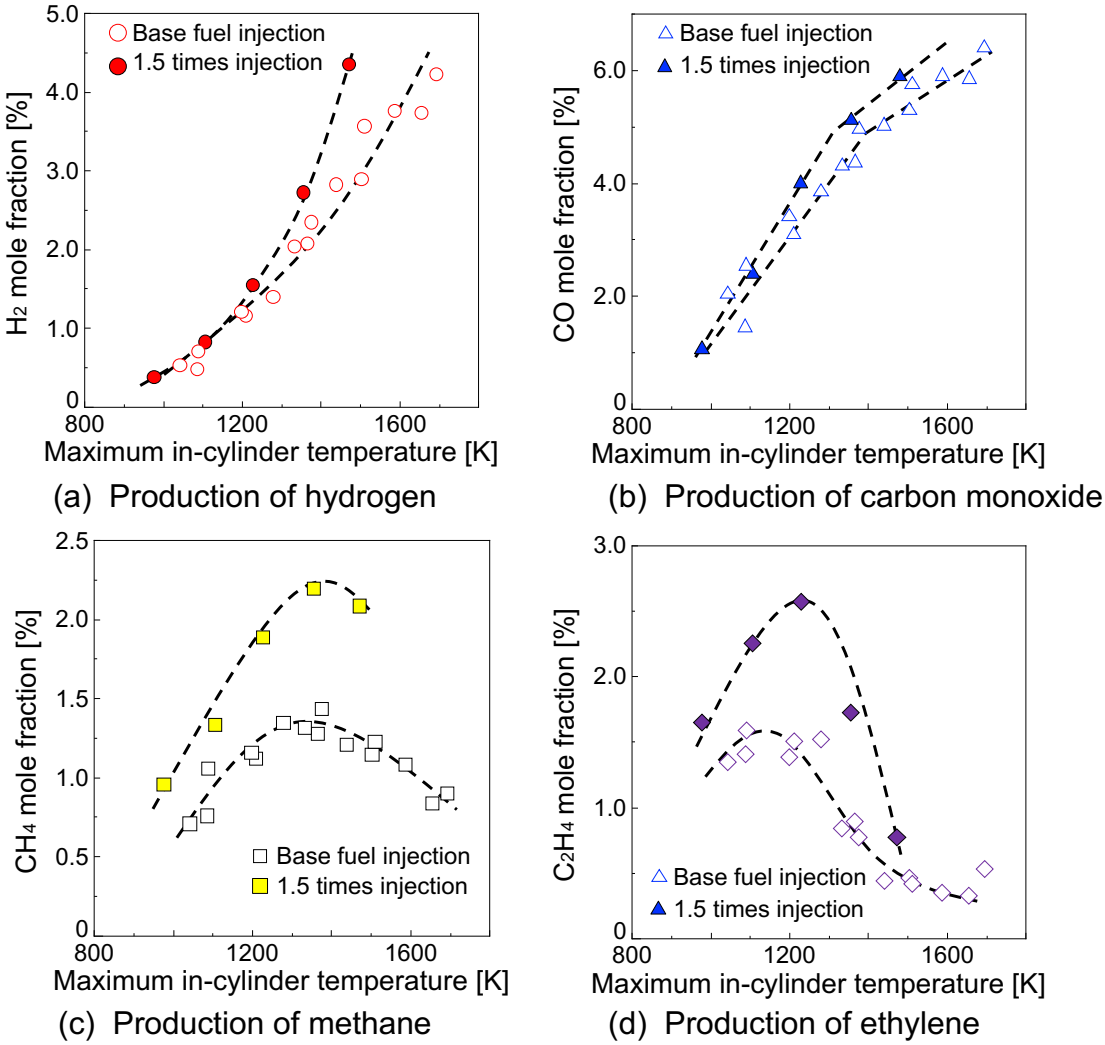

Fig. 9 Effects of 1.5 times fuel injection quantity on reformed gas production (Test 3, for the IDI engine)

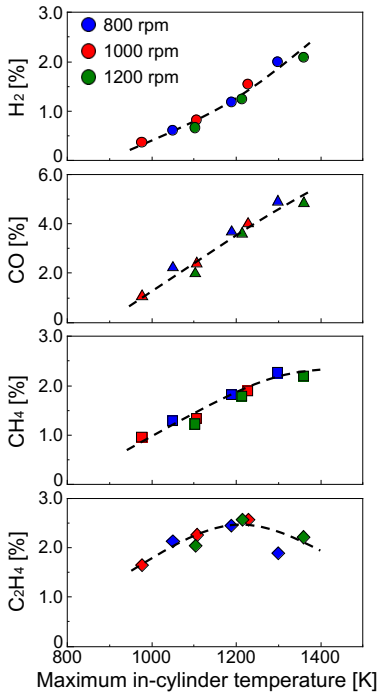

Fig. 10 Effects of engine speed on reformed gas production (Test 4, for the IDI engine)

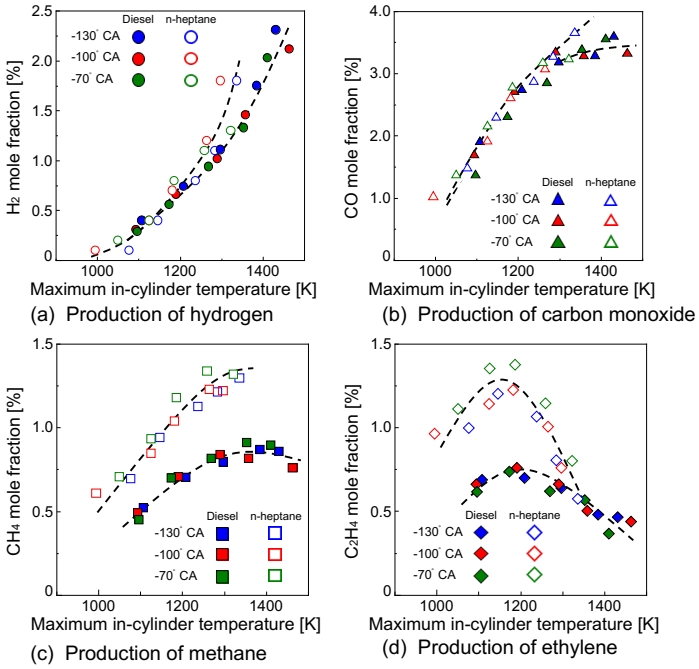

Fig. 11 Effects of fuel injection timing on reformed gas production (Test 4, for the IDI engine)

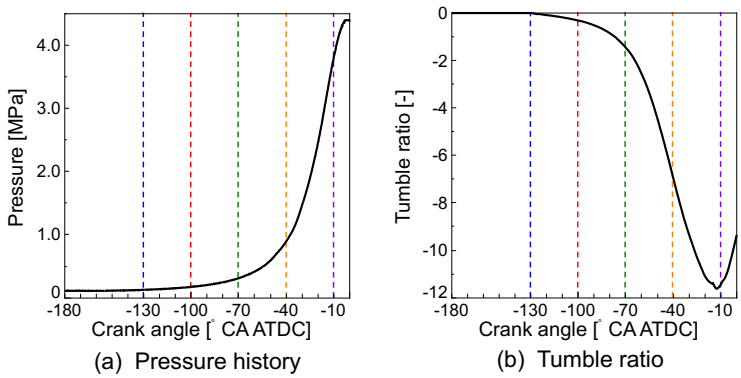

Fig. 12 Histories of pressure and tumble ratios during the compression stroke (calculation)

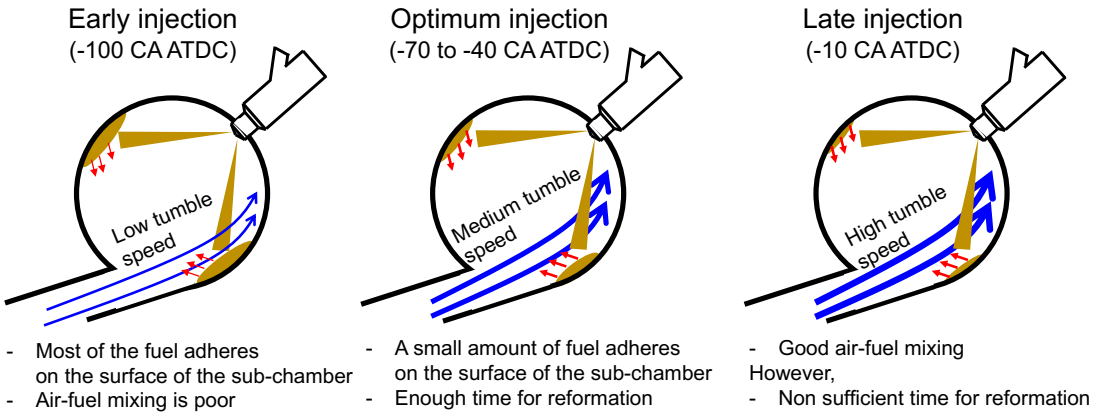

Fig. 13 Fuel adhesion and reformation in the sub-chamber (Test 5)

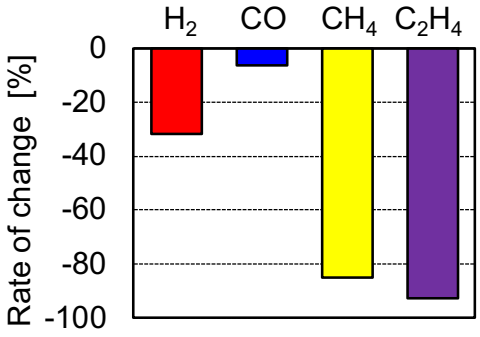

Fig. 14 The results of sensitivity reaction analysis by equation 3: rates of change for hydrogen, carbon monoxide, methane, and ethylene (simulation)

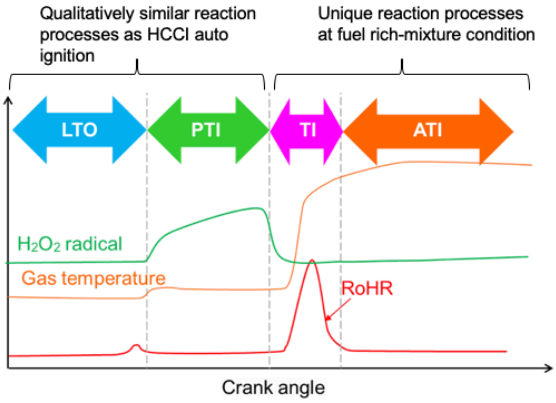

Fig. 15 Four stage reactions in fuel reformation processes

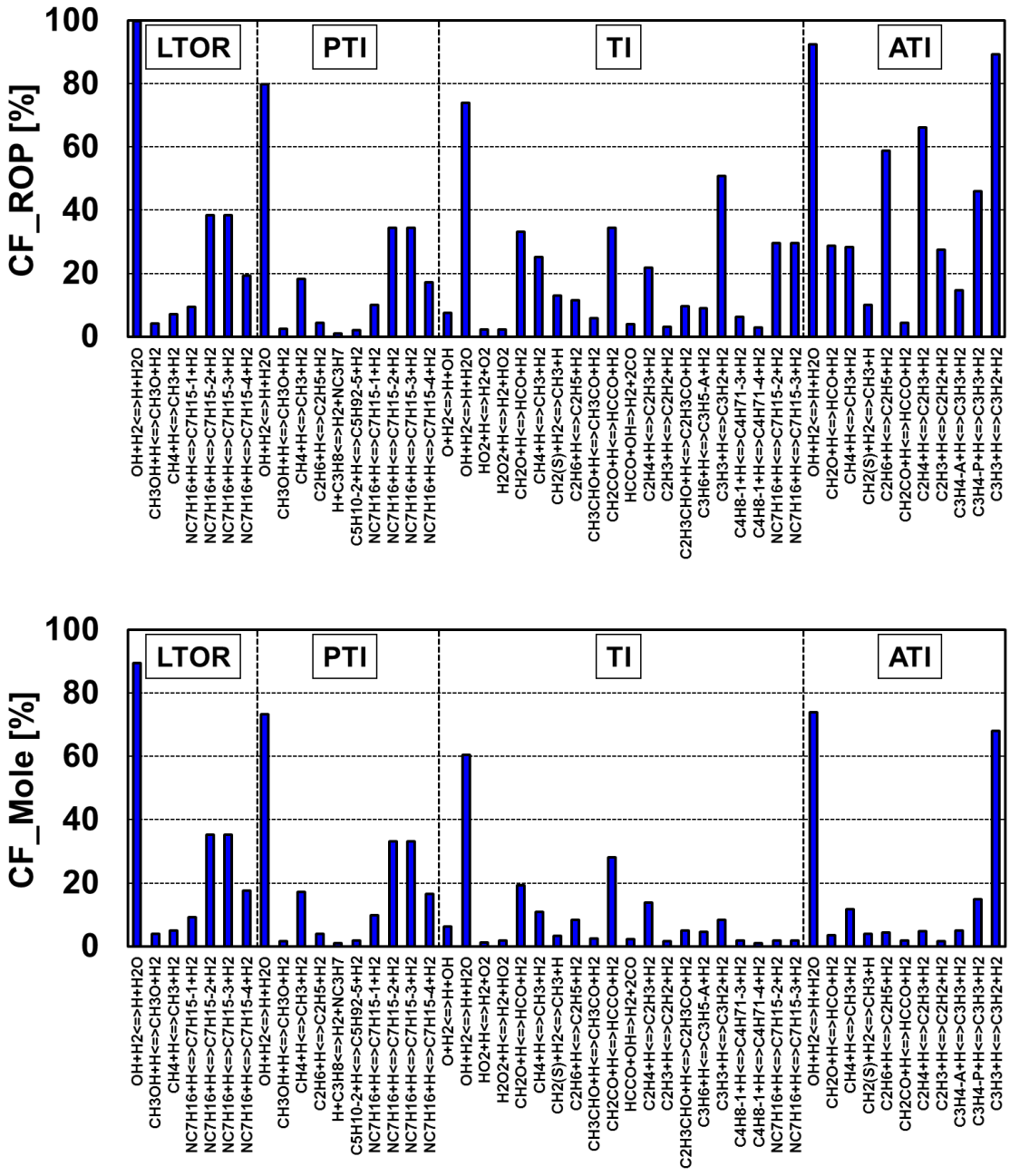

Fig. 16 Contribution factors in hydrocarbon (H_2), top: rate of production (ROP), bottom: mole number

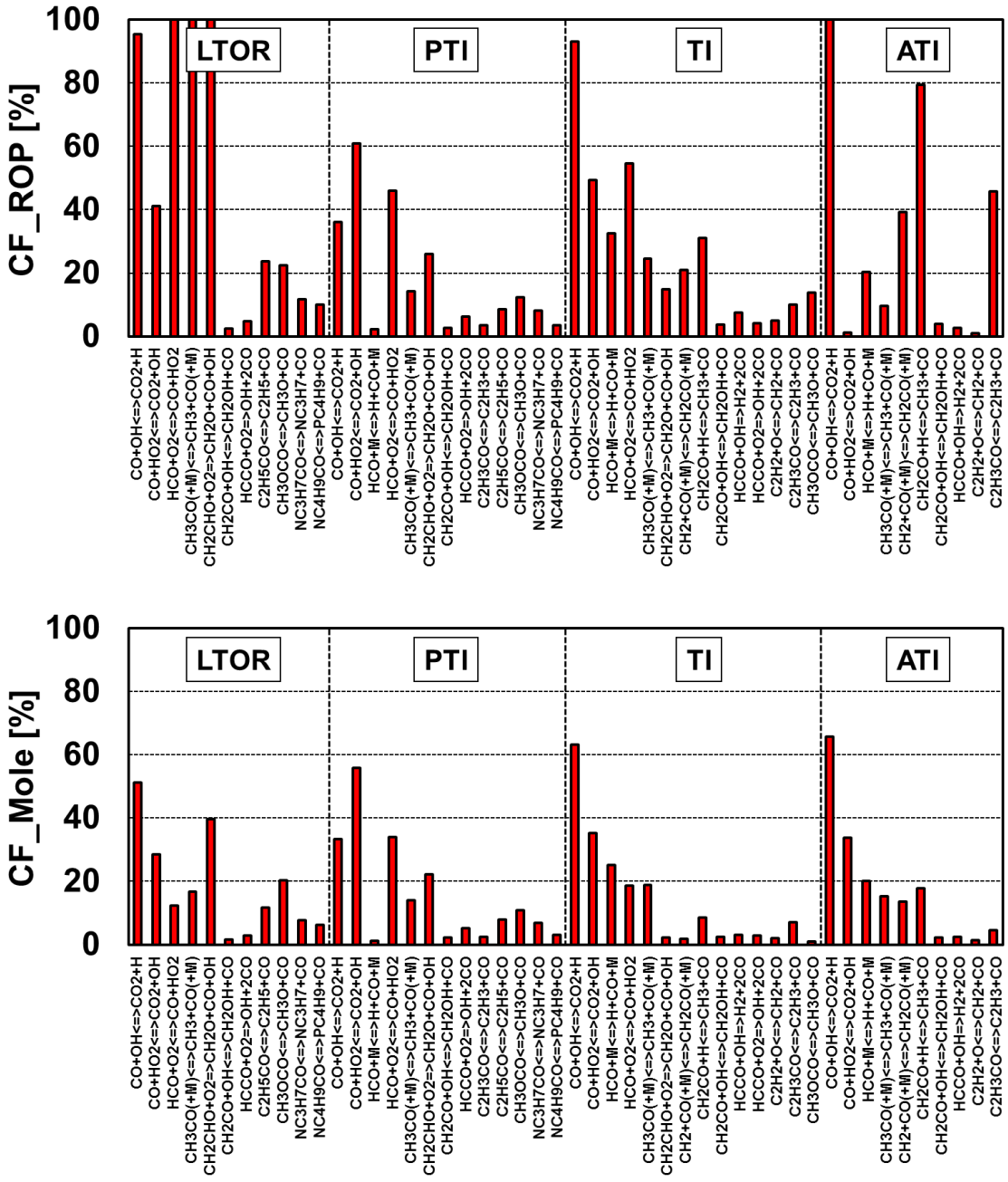

Fig. 17 Contribution factors in carbon monoxide (CO), top: rate of production (ROP), bottom: mole number

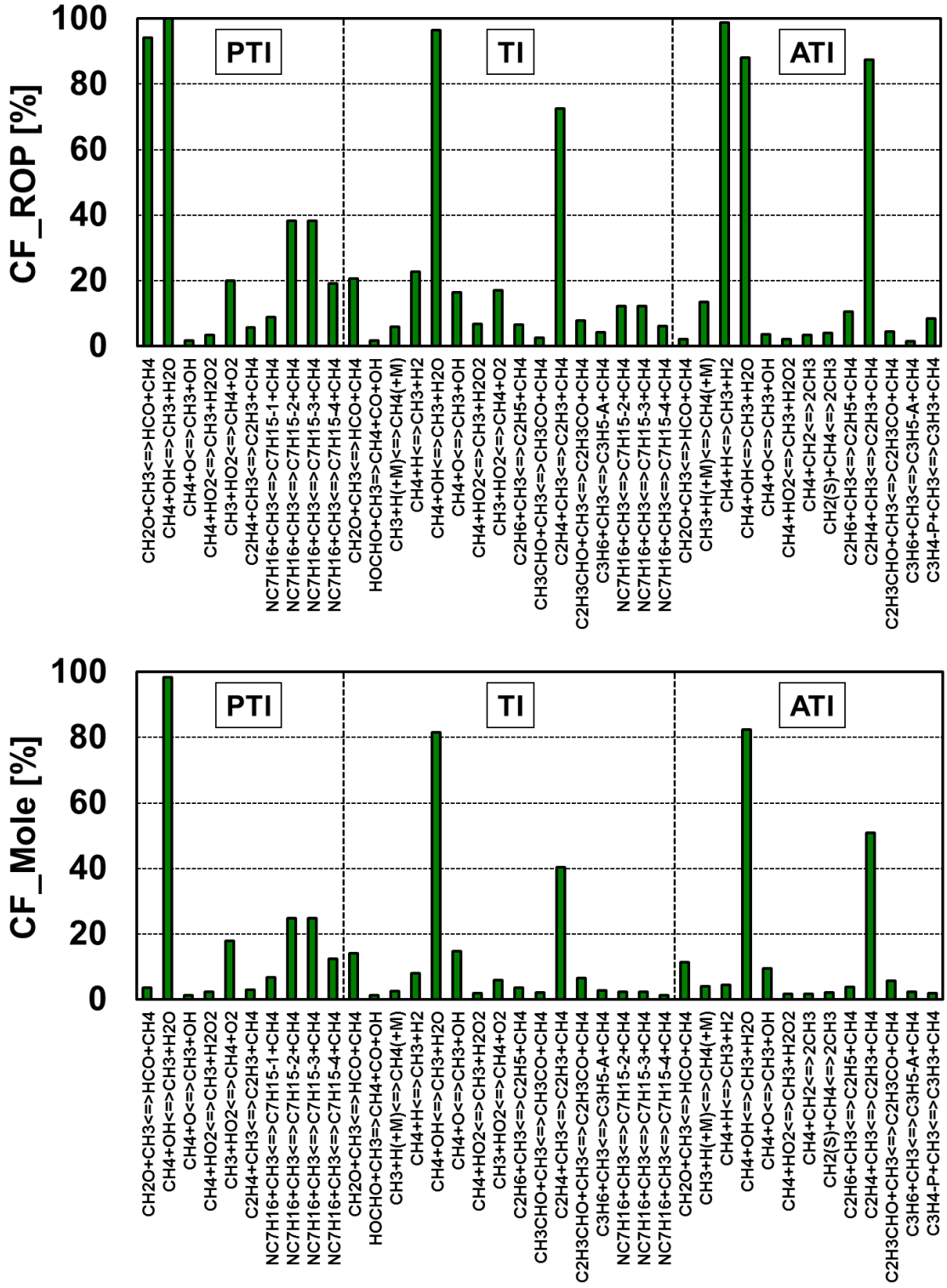

Fig. 18 Contribution factors in methane (CH_4), top: rate of production (ROP), bottom: mole number

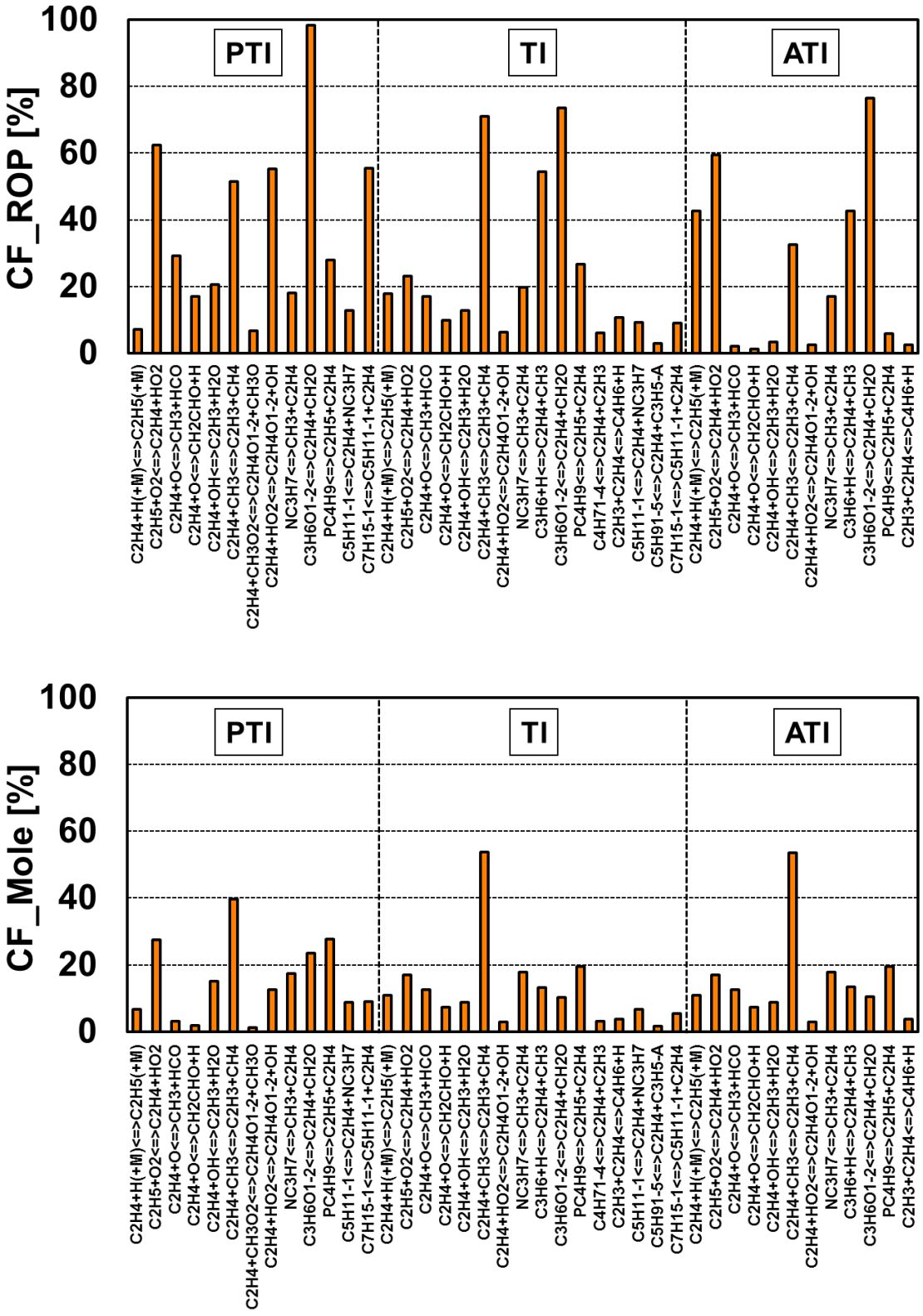

Fig. 19 Contribution factors in ethylene (C_2H_4), top: rate of production (ROP), bottom: mole number

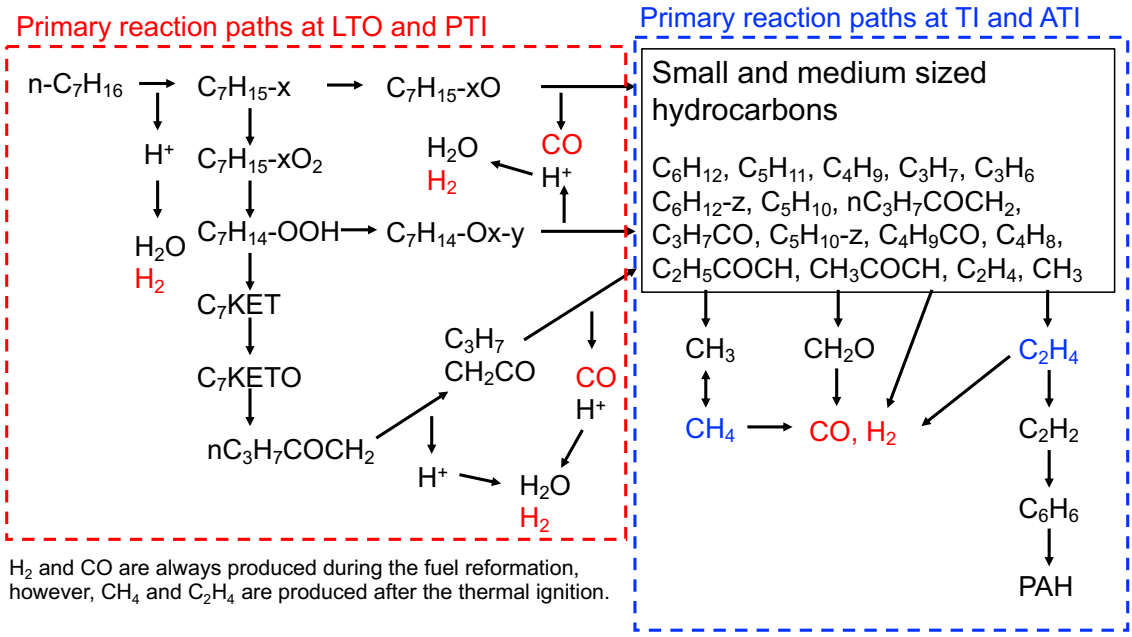

Fig. 20 Fuel reformation processes of n-heptane (simulation)

Table 1 Calculation conditions of CHEMKIN Pro simulation (Base engine: Nissan SC-77)

Solver	-	CHEMKIN Pro
Reactor model	-	Closed internal combustion HCCI engine
Bore	[mm]	85.0
Stroke	[mm]	88.0
Compression ratio		18:1
Engine speed	[rpm]	1000
Fuel	-	n-Heptane (C7H16)
Initial pressure	[kPa (abs)]	101.3
Equivalent ratio	-	1.0 to 8.0
Intake air temperature before compression	[K]	300 to 600 K

Table 2 Analysis conditions of the reformation processes by CHEMKIN Pro

Engine model	HCCI	Engine speed	1000 rpm
Fuel	n-Heptane	Initial pressure	101 kPa
Oxidizer	Air	Initial tempreture	500K
Start crank angle	-160 CA ATDC	Compression ratio	18.0:1
End crank angle	125 CA ATDC	Equivalence ratio	H_2: 2.5
Dispralemdent	499 cm^3		CO: 2.5
			CH_4: 5.0
			C_2H_4: 8.0

Table 3 Test engine specifications

Engine		SC-77 (Nissan)	TF120V-E (Yanmar)
Engine type		HCCI engine	IDI diesel engine
Number of cylinder		Single cylinder	Single cylinder
Bore	[mm]	85.0	92.0
Stroke	[mm]	88.0	96.0
Displacement	[cm^3]	499	638
Compression ratio		18:1 (Base)	19.4:1

Table 4　Test conditions for Test 1 (Fundamental fuel reformation tests by the HCCI engine) (n-heptane)

Engine speed [rpm]	Compression ratio [-]	Intake air temperature [K]	Oxygen concentration [vol %]	Equivalence ratio [-]
1000	16.0	400	10.0	2.0
			8.0	2.5
			6.0	3.3
		450	10.0	2.0
			8.0	2.5
			6.0	3.3
		500	10.0	2.0
			8.0	2.5
			6.0	3.3
	18.0	400	10.0	2.0
			8.0	2.5
			6.0	3.3
		450	10.0	2.0
			8.0	2.5
			6.0	3.3
		500	10.0	2.0
			8.0	2.5
			6.0	3.3
	20.0	400	8.0	2.5
			6.0	3.3
			4.0	5.0
		450	8.0	2.5
			6.0	3.3
			4.0	5.0
		500	8.0	2.5
			6.0	3.3
			4.0	5.0

Table 5　Test conditions for Test 2 (Fundamental fuel reformation tests by the IDI engine) (n-heptane)

Engine speed [rpm]	Compression ratio [-]	Intake air temperature [K]	Oxygen concentration [vol %]	Equivalent ratio [-]
1000	19.4	400	8.0	2.5
			7.0	2.9
			6.0	3.3
			5.0	4.0
			4.0	5.0
		450	8.0	2.5
			7.0	2.9
			6.0	3.3
			5.0	4.0
			4.0	5.0
		500	8.0	2.5
			7.0	2.9
			6.0	3.3
			5.0	4.0
			4.0	5.0

Table 6　Test conditions for Test 3 (Effects of fuel injection quantity on reformed gas production) (IDI engine) (n-heptane)

Engine speed [rpm]	Compression ratio [-]	Intake air temperature [K]	Oxygen concentration [vol %]	Equivalence ratio (Base)	Eauivalence ratio (1.5 times)
1000	19.4	500	8.0	2.5	3.8
			7.0	2.9	4.3
			6.0	3.3	5.0
			5.0	4.0	6.0
			4.0	5.0	7.5

Table 7 Test conditions for Test 4 (Effects of engine speed on reformed gas production) (n-heptane)

Engine speed [rpm]	Compression ratio [-]	Intake air temperature [K]	Oxygen concentration [vol %]	Equivalence ratio [-]
800	19.4	500	6.0	5.0
			5.0	6.0
			4.0	7.5
1000	19.4	500	6.0	5.0
			5.0	6.0
			4.0	7.5
1200	19.4	500	6.0	5.0
			5.0	6.0
			4.0	7.5

Table 8 Diesel fuel properties

Boiling point	[C]	176-348
Density	[kg/m^3]	834.6
Lower heating value	[MJ/kg]	43.3
Cetane number		54.5

Table 9 Test conditions for Test 5 (Effects of fuel injection timing on reformed gas production) (IDI engine) (Diesel fuel and n-heptane)

Engine speed [rpm]	Compression ratio [-]	Intake air temperature [K]	Fuel injection timing [CA ATDC]	Oxygen concentration [vol %]	Equivalence ratio [-]
1000	19.4	500	-130	8.0	2.5
				7.0	2.9
				6.0	3.3
				5.0	4.0
				4.0	5.0
			-100	8.0	2.5
				7.0	2.9
				6.0	3.3
				5.0	4.0
				4.0	5.0
			-70	8.0	2.5
				7.0	2.9
				6.0	3.3
				5.0	4.0
				4.0	5.0

Table 10　Reformed gas composition of n-heptane in Test 5

Fuel injection timing [CA ATDC]	Intake O2 conc. %	Maximum temp. [K]	H2 [vol %]	CO [vol %]	CH4 [vol %]	C2H4 [vol %]
-130	8.0	1336	1.8	3.7	1.3	0.6
	7.0	1284	1.1	3.3	1.2	0.8
	6.0	1238	0.8	2.9	1.1	1.1
	5.0	1146	0.4	2.3	0.9	1.2
	4.0	1076	0.1	1.5	0.7	1.0
-100	8.0	1297	1.8	3.2	1.2	0.8
	7.0	1264	1.2	3.1	1.2	1.0
	6.0	1181	0.7	2.6	1.0	1.2
	5.0	1125	0.4	1.9	0.8	1.1
	4.0	995	0.1	1.0	0.6	1.0
-70	8.0	1322	1.3	3.2	1.3	0.8
	7.0	1259	1.1	3.2	1.3	1.1
	6.0	1186	0.8	2.8	1.2	1.4
	5.0	1125	0.4	2.2	0.9	1.4
	4.0	1050	0.2	1.4	0.7	1.1

Table 11　Reformed gas composition of diesel fuel in Test 5

Fuel injection timing [CA ATDC]	Intake O2 conc. %	Maximum temp. [K]	H2 [vol %]	CO [vol %]	CH4 [vol %]	C2H4 [vol %]
-130	8.0	1431	2.3	3.6	0.9	0.5
	7.0	1385	1.8	3.3	0.9	0.5
	6.0	1297	1.1	3.2	0.8	0.6
	5.0	1208	0.7	2.7	0.7	0.7
	4.0	1108	0.4	1.9	0.5	0.7
-100	8.0	1463	2.1	3.3	0.8	0.4
	7.0	1358	1.5	3.3	0.8	0.5
	6.0	1290	1.0	3.3	0.8	0.7
	5.0	1190	0.7	2.7	0.7	0.8
	4.0	1093	0.3	1.7	0.5	0.7
-70	8.0	1411	2.0	3.6	0.9	0.4
	7.0	1353	1.3	3.4	0.9	0.6
	6.0	1269	0.9	2.8	0.8	0.6
	5.0	1173	0.6	2.3	0.7	0.7
	4.0	1096	0.3	1.4	0.4	0.6

Table AP-1 Main reactions of production and consumption of hydrogen (simulation)

	Elementary reactions		Elementary reactions
Production (17)	$CH_4+H <=> CH_3+H_2$	Consumption (10)	$OH+H_2 <=> H+H_2O$
	$nC_7H_{16}+H <=> C_7H_{15}\text{-}1+H_2$		$CH_3OH+H <=> CH_3O+H_2$
	$nC_7H_{16}+H <=> C_7H_{15}\text{-}2+H_2$		$H+C_3H_8 <=> H_2+nC_3H_7$
	$nC_7H_{16}+H <=> C_7H_{15}\text{-}3+H_2$		$C_5H_{10}\text{-}2+H <=> C_5H_9\text{-}2+H_2$
	$nC_7H_{16}+H <=> C_7H_{15}\text{-}4+H_2$		$O+H_2 <=> H+OH$
	$C_2H_6+H <=> C_2H_5+H_2$		$H_2O_2+H <=> H_2+HO_2$
	$HO_2+H <=> H_2+O_2$		$CH_2(S)+H_2 <=> CH_3+H$
	$CH_2O+H <=> HCO+H_2$		$CH_2CO+H <=> HCCO+H_2$
	$CH_3CHO+H <=> CH_3CO+H_2$		$C_3H_4\text{-}A+H <=> C_3H_3+H_2$
	$HCCO+OH <=> H_2+2CO$		$C_3H_4\text{-}P+H <=> C_3H_3+H_2$
	$C_2H_4+H <=> C_2H_3+H_2$		
	$C_2H_3+H <=> C_2H_2+H_2$		
	$C_2H_3CHO+H <=> C_2H_3CO+H_2$		
	$C_3H_6+H <=> C_3H_5+H_2$		
	$C_3H_3+H <=> C_3H_2+H_2$		
	$C_4H_8\text{-}1+H <=> C_4H_71\text{-}3+H_2$		
	$C_4H_8\text{-}1+H <=> C_4H_71\text{-}4+H_2$		

$RH + H <=> R + H_2$
Dehydrogenation

Table AP-2 Main reactions of production and consumption of carbon monoxide (simulation)

	Elementary reactions		Elementary reactions
Production (14)	$HCO+O_2 <=> CO+HO_2$	Consumption (3)	$CO+OH <=> CO_2+H$
	$CH_3CO(+M) <=> CH_3+CO(+M)$		$CO+HO_2 <=> CO_2+OH$
	$CH_2CHO+O_2 <=> CH_2O+CO+OH$		$CH_3OCO <=> CH_3O+CO$
	$CH_2CO+OH <=> CH_2OH+CO$		
	$HCCO+O_2 <=> OH+2CO$		
	$C_2H_5CO <=> C_2H_5+CO$		
	$nC_3H_7CO <=> nC_3H_7+CO$		
	$nC_4H_9CO <=> nC_4H_9+CO$		
	$HCO+M <=> H+CO+M$		
	$C_2H_3CO <=> C_2H_3+CO$		
	$CH_2+CO(+M) <=> CH_2CO(+M)$		
	$CH_2CO+H <=> CH_3+CO$		
	$HCCO+OH <=> H_2+2CO$		
	$C_2H_2+O <=> CH_2+CO$		

$RCO <=> R + CO$
Dissociation of carbonyl radical

Table AP-3 Main reactions of production and consumption of methane (simulation)

	Elementary reactions		Elementary reactions
Production (13)	$CH_2O+CH_3 <=> HCO+CH_4$	Consumption (7)	$CH_4+OH <=> CH_3+H_2O$
	$CH_3+HO_2 <=> CH_4+O_2$		$CH_4+O <=> CH_3+OH$
	$C_2H_4+CH_3 <=> C_2H_3+CH_4$		$CH_4+HO_2 <=> CH_3+H2O_2$
	$nC_7H_{16}+CH_3 <=> C_7H_{15}\text{-}1+CH_4$		$CH_4+H <=> CH_3+H_2$
	$nC_7H_{16}+CH_3 <=> C_7H_{15}\text{-}2+CH_4$		$CH_4+CH_2 <=> 2CH_3$
	$nC_7H_{16}+CH_3 <=> C_7H_{15}\text{-}3+CH_4$		$CH_2(S)+CH_4 <=> 2CH_3$
	$nC_7H_{16}+CH_3 <=> C_7H_{15}\text{-}4+CH_4$		$C_3H_4+CH_3 <=> C_3H_3+CH_4$
	$HOCHO+CH_3 <=> CH_4+CO+OH$		
	$CH_3+H(+M) <=> CH_4(+M)$		
	$C_2H_6+CH_3 <=> C_2H_5+CH_4$		
	$CH_3CHO+CH_3 <=> CH_3CO+CH_4$		
	$C_2H_3CHO+CH_3 <=> C_2H_3CO+CH_4$		
	$C_3H_6+CH_3 <=> C_3H_5+CH_4$		

Dehydrogenation by methyl radical
$RH + CH_3 <=> R + CH_4$

Table AP-4 Main reactions of production and consumption of ethylene (simulation)

	Elementary reactions		Elementary reactions
Production (9)	$C_2H_4+H(+M) <=> C_2H_5(+M)$	Consumption (8)	$C_2H_4+O <=> CH_3+HCO$
	$C_2H_5+O_2 <=> C_2H_4+HO_2$		$C_2H_4+O <=> CH_2CHO+H$
	$nC_3H_7 <=> CH_3+C_2H_4$		$C_2H_4+OH <=> C_2H_3+H_2O$
	$C_4H_9 <=> C_2H_5+C_2H_4$		$C_2H_4+CH_3 <=> C_2H_3+CH_4$
	$C_5H_{11} <=> C_2H_4+nC_3H_7$		$C_2H_4+CH_3O_2 <=> C_2H_4O+CH_3O$
	$C_7H_{15} <=> C_5H_{11}+C_2H_4$		$C_2H_4+HO_2 <=> C_2H_4O+OH$
	$C_3H_6+H <=> C_2H_4+CH_3$		$C_3H_6O <=> C_2H_4+CH_2O$
	$C_4H_7 <=> C_2H_4+C_2H_3$		$C_2H_3+C_2H_4 <=> C_4H_6+H$
	$C_5H_9 <=> C_2H_4+C_3H_5$		

Thermal decomposition
of higher hydrocarbons

$$R \rightleftarrows R' + C_2H_4$$